

## Catalytic upgrading of pyrolysis vapours: Effect of catalyst support and metal type on phenolic content of bio-oil



Elif Yaman <sup>a,\*</sup>, Adife Seyda Yargic <sup>b</sup>, Nurgul Ozbay <sup>b</sup>, Basak Burcu Uzun <sup>c</sup>,  
Konstantinos G. Kalogiannis <sup>d</sup>, Stylianos D. Stefanidis <sup>d</sup>, Eleni P. Pachatouridou <sup>d</sup>,  
Eleni F. Iliopoulou <sup>d</sup>, Angelos A. Lappas <sup>d</sup>

<sup>a</sup> Bilecik Seyh Edebali University, Central Research Laboratory, 11210, Bilecik, Turkey

<sup>b</sup> Bilecik Seyh Edebali University, Department of Chemical and Process Engineering, 11210, Bilecik, Turkey

<sup>c</sup> Anadolu University, Department of Chemical Engineering, 26470, Eskişehir, Turkey

<sup>d</sup> Centre for Research and Technology Hellas, Chemical Process and Energy Resources Institute, 57001 Thessaloniki, Greece

### ARTICLE INFO

#### Article history:

Available online 5 March 2018

#### Keywords:

Acid pre-treatment  
Bio-oil  
Catalytic pyrolysis  
Catalyst type  
Phenolic contents  
Walnut shell

### ABSTRACT

Bio-oil from low-cost and renewable lignocellulosic biomass is a complex mixture of organic compounds and water. It is necessary to selectively control the biomass pyrolysis pathways to obtain specific bio-oils rich in value-added chemicals. Microporous and mesoporous catalysts can be good candidates for the catalytic pyrolysis of biomass leading to the production of valuable components such as aromatic hydrocarbons and phenolics. In this study, in-situ catalytic upgrading of pyrolysis vapours from acid pre-treated walnut shell was carried out in a lab scale fixed bed reactor with microporous nickel or cobalt impregnated Zeolite Socony Mobil-5 and mesoporous aluminum or iron impregnated Santa Barbara Amorf-15 catalysts. The effects of catalyst modification on product yields, bio-oil quality and the variation of the phenolic compounds in pyrolytic-oil were examined using elemental analysis, gas chromatography and mass spectrometry. The major improvement in the bio-oil quality by the catalyst addition was the reduction of the oxygen content of the bio-oil's organic fraction and the increase in valuable chemicals (aromatics and phenolics), while the total liquid yield (bio-oil) decreased. Catalysts also increased the gaseous product yields. In comparison to non-catalytic experiments, all the Proton-exchanged Zeolite Socony Mobil-5 catalysts decreased both the total liquid and the total organic content yield due to the H<sup>+</sup>-form zeolite catalysing hydrocarbon conversion reactions. Compared to Proton-exchanged Zeolite Socony Mobil-5, the metal impregnated catalysts yielded less water, but favoured the formation of gas products. It was evident that impregnation with metals changed the mechanism of oxygen removal. Cobalt/Proton-exchanged Zeolite Socony Mobil-5 favoured the formation of carbon dioxide over carbon monoxide, while nickel/Proton-exchanged Zeolite Socony Mobil-5 favoured the formation of carbon monoxide over carbon dioxide. When using Proton-exchanged Zeolite Socony Mobil-5 instead of silica sand, the guaiacols and syringol that are formed from the thermal decomposition of the lignin fraction in the sulphuric acid treated walnut shell are significantly reduced and are mainly converted to alkylated phenols and aromatic and polyaromatic hydrocarbons. With the impregnation of metals on the Santa Barbara Amorf-15, the selectivity of the Santa Barbara Amorf-15 exhibited a shift from catechol- and pyrogallols-type compounds to alkylated phenols, especially at 10% aluminum, 30% and 50% iron metal loadings. As a result, the bio-oil composition and quality can be improved by utilizing different metals and metal impregnation ratios during catalytic upgrading. According to the preliminary economic analysis, pyrolysis oil production cost predicted from catalytic pyrolysis of walnut shell is higher than catalytic pyrolysis of woody biomass because of lower pyrolysis oil yield of walnut shell.

© 2018 Elsevier Ltd. All rights reserved.

\* Corresponding author.

E-mail addresses: [elif.yaman@bilecik.edu.tr](mailto:elif.yaman@bilecik.edu.tr) (E. Yaman), [seyda.guler@bilecik.edu.tr](mailto:seyda.guler@bilecik.edu.tr) (A.S. Yargic), [nurgul.ozbay@bilecik.edu.tr](mailto:nurgul.ozbay@bilecik.edu.tr) (N. Ozbay), [kkgaloga@cperi.certh.gr](mailto:kkgaloga@cperi.certh.gr) (K.G. Kalogiannis), [s\\_stepha@cperi.certh.gr](mailto:s_stepha@cperi.certh.gr) (S.D. Stefanidis), [eh@cperi.certh.gr](mailto:eh@cperi.certh.gr) (E.P. Pachatouridou), [angel@cperi.certh.gr](mailto:angel@cperi.certh.gr) (A.A. Lappas).

### 1. Introduction

Global warming, limited reserves of fossil fuels and environmental considerations have triggered the search for cleaner

processes and renewable resources (Lim et al., 2016). Renewable energy sources, as an alternative to traditional fossil fuels, have the potential to mitigate energy dependence and reduce pollution resulting from fossil fuel use (Ning et al., 2013). Lignocellulosic biomass, such as forest residues, agro-wastes, energy grasses, aquatic plants and algae, is a non-edible renewable energy source that does not compete with food production and can be converted into value added fuels or fuel precursors, biochemicals and other products (Mohammed et al., 2017). Research on the environmental impact of biomass has shown that it is a promising energy resource for development of a sustainable energy future (Balasundram et al., 2017).

Pyrolysis is one of the most promising methods used for the thermochemical conversion of lignocellulosic biomass and is described as the thermal decomposition of lignocellulosic biomass by heat in an oxygen-free atmosphere, which generates solid, liquid and gaseous products. Lignocellulosic biomass such as tea waste (Uzun et al., 2010), Japanese cedar wood (Kumagai et al., 2015), olive stone, almond shell, pine wood, olive-tree pruning (Gomez et al., 2016) Bambara groundnut shell (Mohammed et al., 2016) and tomato waste (Ozbay et al., 2017) is composed primarily of cellulose, hemicellulose and lignin, as well as minor amounts of other organics. One advantage of pyrolysis is that it can handle whole biomass, unlike hydrothermal and biochemical processes that require the separation of lignin from the hemicellulose and cellulose fractions. Lignin is a heterogeneous, complex, three-dimensional polymer, composed of methoxy and hydroxyl substituted phenyl-propane units and as such, it is a natural renewable resource of aromatic compounds. Fast pyrolysis of lignin forms many non-volatile oligomers (such as pyrolytic lignins, mainly tri- and tetramers) and volatile phenolic compounds, while the thermal decomposition of the cellulose and hemicellulose fractions yields a wide array of oxygenated compounds, such as, alcohols, aldehydes, esters, ketones, sugars and furans. Condensation of the above compounds forms the liquid product of pyrolysis, known as bio-oil, which can be used as a fuel, fuel-precursor or as a source of high added value chemicals (Aysu, 2015). Bio-oil is considered to be a very promising biofuel/bioenergy carrier that can be easily transported and utilized as fuel for stationary power applications or alternatively, it can be refined in conventional petroleum refineries for the production of higher quality light hydrocarbon fuels that can replace petroleum-derived transportation fuels (Huber et al., 2006), which are a significant source of environmental pollution due to  $\text{SO}_x$ ,  $\text{NO}_x$  and  $\text{CO}_2$  emissions. For these reasons, the production of bio-oil has been investigated in pilot and demonstration scale, in an effort to evaluate its economic and environmental sustainability, while a commercial biomass thermal pyrolysis facility has been constructed and operated by Ensyn in Renfrew Ontario, since 2006. In a recent life cycle assessment study, bio-oil was shown to have high energy efficiency, while its environmental impact was estimated to be only 15–18% of that of fossil-fuel oil (Ning et al., 2013). Bio-oil is a complex mixture of molecules with variable molecular weights, ranging from water to oligomeric phenolic compounds (Oasmaa and Czernik, 1999). Its average molecular weight ranges from 370 to 790 and is a function of many parameters, such as feedstock type, pyrolysis temperature and reactor type (Pittman et al., 2012; Hassan et al., 2016). The pyrolytic lignins and oxygenated compounds in the bio-oil cause many unfavourable properties during application, storage, and upgrading. Microporous and mesoporous catalysts have the potential to mitigate these disadvantages by converting large oligomers and oxygenates into more desirable products via catalytic cracking of the pyrolysis vapours (Qiang et al., 2009).

Cellulose, hemicellulose and lignin contain C–O bonds that are responsible for the connections in all units of the macromolecules.

Most of these bonds can be hydrolyzed in the presence of acid, which facilitates the decomposition of lignocellulosic biomass components into smaller compounds by pyrolysis (Kumagai et al., 2015). In the literature, acid pre-treatment is generally applied at high temperature (163–230 °C) and pressure (~10 atm) (Kumar et al., 2009; Iranmahboob et al., 2002). Only a few studies at room temperature and atmospheric pressure of acid pre-treatment can be found, although such a process has several virtues, such as the simplification of equipment and reduction of energy requirements by avoiding unnecessary heating. Acid pre-treatment can also cause a significant removal of the numerous alkali and alkaline earth metals that are contained in biomass. In the literature, acid washing for mineral removal has been applied for various biomass feeds, such as Douglas fir wood (softwood) (Zhou et al., 2013a, 2013b), mallee wood (Mourant et al., 2011), sugarcane bagasse (David et al., 2017) and beech wood (Stefanidis et al., 2015). The metals in the biomass are responsible for catalytic reactions that yield gas products and char at the expense of the desirable liquid organic products, while their removal by acid washing can significantly increase bio-oil yields.

The use of catalysis in the pyrolysis of biomass is an effective approach to improve the quality of the bio-oil and optimize selectivity to desirable compounds. Since biomass exists in a large number of forms, thus having different components and structures, pyrolysis of different biomass species may require different additives/catalysts to optimize the process (Uzun and Sarioglu, 2009). During in-situ catalytic pyrolysis, a heterogeneous catalyst is used in the pyrolysis reactor. The pyrolysis vapours come in contact with the catalyst and are catalytically cracked, deoxygenated and converted to more desirable compounds, such as aromatic hydrocarbons and phenols (Iliopoulou et al., 2014). The main challenge in catalytic cracking is the selection or design of suitable catalysts. An ideal catalyst for the biomass pyrolysis process should produce satisfactory yields of high quality bio-oil with low oxygen content, convert the undesirable compounds present in the pyrolysis vapours to desirable compounds and exhibit both resistance to deactivation and thermal stability (Lappas et al., 2012). Significant modification of the pyrolysis products can be achieved using various catalysts, such as microporous zeolites, mesoporous materials with uniform pore size distribution (SBA-15, MSU, MCM-41), hybrid microporous/mesoporous materials, catalysts doped with noble and transition metals and base catalysts. Solid acidic catalysts, such as zeolites are usually used in catalytic pyrolysis of large hydrocarbon fractions in petroleum refining. During biomass pyrolysis, scission of C–C, C–OH and C–CO(OH) bonds becomes important due to the carbohydrate and phenolic components of cellulose, hemicellulose and lignin. Thereby, dehydration, decarboxylation, cracking, oligomerization and aromatization can occur on the acid sites of zeolites. ZSM-5 significantly changes the composition of bio-oil by both reducing the amount of oxygenated compounds by deoxygenation reactions and simultaneously increasing the aromatic species. Because of the strong acidity of ZSM-5, over cracking towards gases or coke occurs resulting in significant carbon loss and decreased bio-oil yield. Adjustment of acid site availability is an important aspect to the design of solid acid catalysts. Thus, metal promotion of zeolites has been tested and has been found to enhance hydrocarbon yields when using Ce, Co, Al, Fe, Ga, Ni and Co-substituted ZSM-5. These metal promoted zeolitic materials with modified acidity, can increase selectivity to hydrocarbons while producing less coke than conventional ZSM-5 (French and Czernik, 2010; Iliopoulou et al., 2012). Recent catalyst development for lignocellulosic biomass conversion has focused on mesoporous materials. SBA-15 is by far the largest pore size mesoporous material

with highly ordered hexagonally arranged mesochannels, thick walls, adjustable pore size from 3 nm to 30 nm, and high hydrothermal stability. These properties make SBA-15 a promising candidate catalyst for treating biomass pyrolysis vapours, which contain a significant amount of steam and large molecules. However, SBA-15 is a purely silica based material that lacks acidity. To create acid sites and improve the catalytic properties, an option is the incorporation of various (Ni, Al, Co, Mo, Fe, Cu) metals in the framework of the mesoporous silica by doping (one-pot synthesis) or post-grafting (Qiang et al., 2009).

In this study, the production of bio-oil from agricultural waste biomass by catalytic pyrolysis and the effect of catalyst support and metal impregnation on the phenolic fraction of the bio-oil have been investigated. Agricultural waste biomass is a renewable energy resource that does not compete with food production and its utilization can contribute to sustainable development via the cleaner production of fuel precursors and high added value chemical products. Waste valorisation is key to reducing the environmental impact of industries such as the agricultural sector. Upgrading and converting agricultural byproducts allows for the cleaner and CO<sub>2</sub> emission neutral production of agricultural products and of high added value fuels and chemicals. Walnut shell (WS) was used as raw material for catalytic bio-oil production with high phenolics content. WS was chosen because of its importance as an agricultural waste, as mentioned above, as well as because of its challenging composition; WS has lower cellulose and hemicellulose content and much higher lignin (~50 wt%) and extractives content than wood (Pirayesh et al., 2013; Zhai et al., 2015). Walnut is an essential crop that is harvested throughout the world's temperate regions for its edible nuts. Worldwide walnut production was approximately 2.2 million tonnes in 2009. In 2012, walnut production was about 203,212 tonnes in Turkey. As the shell of walnut comprises 67% of the total weight of the fruit, around 136,150 tonnes of walnut shell was produced in 2012. WS, which is an annual agricultural waste, is the lignocellulosic material forming the thin endocarp or husk of the walnut fruit (Uzun and Yaman, 2014). WS is a food waste feedstock that is difficult to convert via hydrothermal or biochemical processes due to its high lignin content, it presents however great potential for the production of high added value renewable phenolics. The novelty of this work lies in the direct comparison of metal impregnated microporous (ZSM-5) and mesoporous (SBA-15) acidic catalysts, as well as their parent materials, for the upgrading of pyrolysis vapours from walnut shell. Walnut shell was treated in sulphuric acid solution at room temperature and pressure prior to the pyrolysis experiments to remove minerals, hydrolyze lignin C-O bonds and maximize liquid yields. Nickel or cobalt impregnated ZSM-5 and aluminum or iron impregnated SBA-15 catalysts were studied for the upgrading of pyrolysis vapours from the pre-treated walnut shell in a bench scale fixed bed experimental unit. The metal impregnated HZSM-5 and SBA-15 catalysts were evaluated for their applicability to increase phenolic compounds in bio-oil that could be used as value added chemicals. The preliminary economic analysis was also done to estimate the investment and operating cost of a walnut shell catalytic pyrolysis process.

## 2. Materials and methods

The biomass and catalysts that were used in this study are described in this section, as well as the techniques that were used for their preparation and the determination of their properties. The experimental apparatus for the pyrolysis experiments is also described, along with the analytical methods that were used for the characterization of the pyrolysis products.

### 2.1. Materials

Walnut shell (WS) was chosen as biomass feedstock from Bilecik, located in North West Turkey. WS was air-dried at room temperature and then ground in a high speed rotary cutting mill (8000 rpm) and sieved to give particle size (Dp) fractions of  $224 < Dp < 425 \mu\text{m}$ ,  $425 < Dp < 600 \mu\text{m}$ ,  $600 < Dp < 850 \mu\text{m}$ ,  $850 < Dp < 1250 \mu\text{m}$  and  $1250 < Dp < 1800 \mu\text{m}$ . For all experiments in this study, 425–600  $\mu\text{m}$  sized samples were used. Prior to the pyrolysis experiments, WS was dried at 105 °C for 16 h and kept in a desiccator, therefore all pyrolysis results are reported on a dry feed basis.

### 2.2. Preparation and characterization of acid pre-treated biomass

Initially, 1 M sulphuric acid (H<sub>2</sub>SO<sub>4</sub>) solution was prepared by using 96% pure H<sub>2</sub>SO<sub>4</sub> obtained from Carlo Erba reagents group (Val-de-Reuil, France). 1 g of WS was added to the solution and agitation for 1 h at the room temperature was applied using a magnetic stirrer. After agitation, the samples were washed with ultra-pure water until pH of the supernatant was equal to pH of ultra pure water. After filtration, WS was dried for 24 h at 105 °C. The pre-treated samples were labelled as WSH. Before the pyrolysis experiments, WSH was also dried at 105 °C for 16 h and kept in a desiccator, therefore all pyrolysis results are reported on a dry feed basis.

The weight fractions of volatiles and ash of WS and WSH were determined using American Standard Test Methods (ASTM D 1102-84; ASTM E 897-82). The weight fraction of moisture was measured in Sartorius MA 150 moisture analyzer. The ultimate analysis of WS and WSH was performed in an elemental analyzer (Leco CHN628 Series).

### 2.3. Preparation and characterization of catalytic materials

The parent catalytic materials used for the pyrolysis experiments were a commercial crystalline ZSM-5 zeolite (Zeolyst CBV8014, silica/alumina (SiO<sub>2</sub>/Al<sub>2</sub>O<sub>3</sub>) molar ratio = 80) and a SBA-15 material synthesized in the lab using triblock copolymer EO20PO70EO20 (Pluronic P123) as organic template. ZSM-5 was used in proton form and it was further promoted with 5 wt% Ni or Co via dry impregnation. Nitric salts, (nickel(II)nitrate hexahydrate Ni(NO<sub>3</sub>)<sub>2</sub>·6(H<sub>2</sub>O) and cobalt(II)nitrate hexahydrate Co(NO<sub>3</sub>)<sub>2</sub>·6(H<sub>2</sub>O)), were used as the metal sources. After impregnation, the catalysts were calcined at 600 °C for 5 h under air atmosphere. SBA-15 was also further promoted with Al (5 and 10 wt%) or Fe (30 and 50 wt%) via a typical wet impregnation method using aqueous solutions of aluminum chloride (AlCl<sub>3</sub>, 98%, Fluka) and iron(III)nitrate nonahydrate (Fe(NO<sub>3</sub>)<sub>3</sub>·9H<sub>2</sub>O, Merck) salts (Jeon et al., 2013). After impregnation, the metal promoted SBA-15 catalysts were calcined at 550 °C for 5 h under air atmosphere with a heating rate of 5 °C/min. The catalysts were pelletized and crushed into particles of 90–180  $\mu\text{m}$  for characterization and experiments. The catalytic materials were characterized by: i) Inductive coupled plasma-atomic emission spectroscopy (ICP-AES) for the determination of their elemental composition (Ni, Co, Al or Fe for the metal-modified catalyst), using a 4300 DV PerkinElmer Optima spectrometer. ii) X-ray diffraction (XRD) measurements were performed for the ZSM-5 catalysts using a SIEMENS D-500 diffractometer employing CuK $\alpha$ <sub>1</sub> radiation ( $\lambda = 0.15405 \text{ nm}$ ) operating at 40 kV and 30 mA. The XRD patterns were accumulated in the range of 5–75° 2 $\theta$  every 0.02° (2 $\theta$ ) with counting time 2 s per step. XRD for the determination of the mesophases of SBA-15 materials were performed using a PANalytical X'Pert Pro Materials Research Diffractometer employing CuK $\alpha$  radiation ( $\lambda = 0.15405 \text{ nm}$ ), in the range of 0–80° 2 $\theta$  at a scan

rate of 2°/min. *iii*) BET surface area (Brunauer-Emmett-Teller BET method), pore volume and pore size distribution (Barrett-Joyner-Halenda BJH method) were measured by N<sub>2</sub> adsorption-desorption experiments. The experiments were conducted at –196 °C, using an Automatic Volumetric Sorption Analyzer (Autosorb-1MP, Quantochrome). The samples were previously outgassed overnight at 350 °C under vacuum.

#### 2.4. Pyrolysis experiments

The catalytic pyrolysis experiments were performed at 500 °C using a bench scale fixed bed tubular reactor made of stainless steel 316 (ID 1.4 cm, height 36 cm), heated by a 3-zone electrical furnace. The reactor was filled with 0.70 g silica sand or 0.50 g catalyst for the non-catalytic and catalytic experiments, respectively. Silica sand was used as inert solid heat carrier for comparison purposes. The WSH (1.5 g) was loaded in a specially designed piston, which was located outside of the furnace. When the reactor temperature reached 500 °C (measured with a thermocouple at the height of the catalyst bed), WSH was introduced with the aid of the piston in the hot zone of the reactor. The pyrolysis vapours were passed through the catalyst bed with the help of a 100 cm<sup>3</sup>/min nitrogen (N<sub>2</sub>) flow. The gaseous products left from the reactor's bottom and were condensed in a glass receiver immersed in a cooling bath (–17 °C). Non-condensable gases were collected in a gas collection system and their total volume was measured by liquid displacement. Fig. 1 presents a schematic diagram of the experimental set-up. A more detailed description of the experimental setup and procedure can be found in previous studies (Stefanidis et al., 2011a, Iliopoulou et al., 2012).

The amount of charcoal and coke-on-catalyst formed by thermal and/or catalytic cracking was determined by direct weighing. Karl-Fischer titration method (ASTM E203-08) was used to determine the water content of bio-oil, while the carbon and hydrogen content was determined with an elemental analyzer (Leco CHN628 Series). The water/aqueous phase present in the bio-oil was separated from the organic phase using dichloromethane and the organic phase was analyzed in an Agilent 7890A/5975C gas chromatography-mass spectroscopy (GC-MS) system (Electron energy 70 eV; Emission 300 V; Helium flow rate: 0.7 mL/min; Column: HP-5MS; 30 m × 0.25 mm ID × 0.25 μm). For the identification of the compounds in the bio-oil, the NIST 05 spectral library

was used. The gaseous products were analyzed in a HP 5890 Series II gas chromatograph equipped with four columns (Precolumn: OV-101; Columns: Porapak N, Molecular Sieve 5A and Rt-Qplot (30 m × 0.53 mm ID) and two detectors (Thermal Conductivity Dedector-TCD and Flame Ionization Dedector-FID). Pyrolysis experiments were carried out three times under the same conditions for each catalytic material in order to ensure repeatability and the average values from the three experimental runs were used.

### 3. Results and discussion

In this section, results from the characterization of the biomass feedstocks and catalytic materials, as well as from the pyrolysis experiments and product characterization are presented and discussed.

#### 3.1. Effects of acid washing on the chemical structure of samples

The results of proximate and ultimate analyses before and after acid pre-treatment of walnut shell are listed in Table 1. Proximate analysis showed a significant difference between WS and WSH. Lower moisture and ash contents and higher volatile matter content were recorded for WSH compared to WS. In addition, acid pre-treatment resulted in the removal of minerals, as indicated by the lower ash content of WSH. According to ultimate analysis, carbon content of WS increased, while oxygen content decreased after application of the acidic pre-treatment. Higher heating value of WS, calculated using Dulong's formula on ultimate analysis data (Harker and Backhurst, 1981), increased from 17.20 MJ/kg to 19.44 MJ/kg after acid pre-treatment.

#### 3.2. Physicochemical characteristics of catalytic materials

The parent HZSM-5 zeolite, SBA-15 and metal loaded catalysts were characterized by a number of techniques in order to determine the effect of metal addition on the catalyst properties. The physicochemical properties of the microporous and mesoporous catalytic materials used in the catalytic upgrading of biomass fast pyrolysis vapours are given in Table 2. ICP-AES analyses showed that both the parent HZSM-5 and SBA-15 materials were successfully impregnated with metals. As it can be seen in Table 2, actual metal loading on the catalysts, as measured by ICP-AES, was lower than the expected nominal values corresponding to the amounts added during the impregnation process. Some difference between nominal and actual metal loadings is acceptable and expected during the impregnation technique, especially at high metal loadings, due to e.g. solubility of the precursor but most importantly due to partial loss of the salt solution in the beakers, burette and

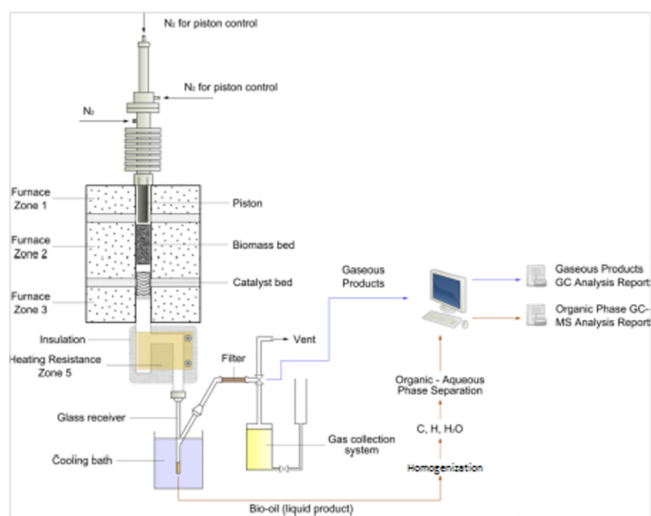


Fig. 1. Schematic representation of the experimental set up for pyrolysis of biomass (Stefanidis et al., 2011b).

Table 1  
Proximate and ultimate analysis of WS and WSH.

Analysis	WS	WSH
<b>Proximate analysis</b>		
Moisture (wt.%)	8.06	2.98
Ash (wt.%)	0.33	0.05
Volatile matter (wt.%)	76.38	83.42
Fixed carbon <sup>a</sup>	15.23	13.55
<b>Ultimate Analysis<sup>b</sup></b>		
C (wt.%)	47.51	50.26
H (wt.%)	6.48	6.97
N (wt.%)	0.47	0.53
O <sup>a</sup> (wt.%)	45.54	42.24
HHV (MJ/kg)	17.20	19.44

<sup>a</sup> Estimated by difference.

<sup>b</sup> Weight percentage on dry basis.

**Table 2**  
Physicochemical properties of catalysts.

	Chemical composition (ICP-AES)		Porosity characteristics (N <sub>2</sub> porosimetry)			
	Nominal metal loading (%)	Actual metal loading (%)	S <sub>BET</sub> <sup>a</sup> (m <sup>2</sup> /g)	Pore size <sup>b</sup> (nm)	V <sub>micro</sub> <sup>c</sup> (cm <sup>3</sup> /g)	V <sub>meso/macro</sub> <sup>d</sup> (cm <sup>3</sup> /g)
HZSM-5	—	—	417.54	3.1	0.126	0.122
5%-Co-HZSM-5	5	5.1 ± 0.3	367.63	2.8	0.116	0.070
5%-Ni-HZSM-5	5	4.9 ± 0.2	368.75	3.0	0.120	0.067
SBA-15	—	—	564.28	4.1	0.027	0.850
5%-Al/SBA-15	5	4.8 ± 0.2	520.25	4.7	0.030	0.886
10%-Al/SBA-15	10	8.9 ± 0.4	456.98	4.8	0.026	0.780
30%-Fe/SBA-15	30	27.7 ± 1.0	352.66	4.7	0.019	0.591
50%-Fe/SBA-15	50	43.0 ± 2.0	233.65	5.5	0.014	0.460

<sup>a</sup> Multi point BET surface area.

<sup>b</sup> Determined by BJH method from nitrogen adsorption data.

<sup>c</sup> From V-t plot analysis.

<sup>d</sup> From the difference of total pore volume at P/P0 = 0.99 minus the micropore volume. S<sub>BET</sub>: Specific BET surface area, (m<sup>2</sup>/g) V<sub>micro</sub>: Specific micropore volume, (cm<sup>3</sup>/g) V<sub>meso/macro</sub>: Specific meso/macro pore volume, (cm<sup>3</sup>/g).

other lab equipment used during the catalyst synthesis. It may be also affected by additional possible experimental errors and the standard deviation of the ICP technique.

For both Co/HZSM-5 and Ni/HZSM-5, the meso/macropore volume was significantly reduced, compared to the micropore volume, which was only slightly affected. This could be an indication that the metal particles were deposited primarily on the external surface of the zeolite, tentatively reducing external surface acidity, which is important for the cracking of large biomass molecules. The specific BET surface area of SBA-15 was 564.28 m<sup>2</sup>/g and impregnation of SBA-15 with metals had a considerable effect on its porosity characteristics. A significant loss of the pore volume and surface area after metal loading was observed, due to the blockage of SBA-15 pores by the metal phases (Iliopoulou et al., 2012). The micropore volume of these catalysts was significantly lower than meso/macropore volumes. Mean pore diameters of catalysts were between 2.8 nm and 3.1 nm for HZSM-5 type and between 4.1 nm and 5.5 nm for SBA-15 type catalysts. The variation of the catalysts' average pore size and surface area after impregnation with metals was expected due to the metal particles blocking some of the catalyst pores and could not be completely avoided, especially at the highest metal loadings that were used (30% and 50% Fe). On one hand, blockage of the pores and reduction of the total surface area of the catalyst is detrimental for its activity, but on the other hand the presence of metals was expected to create new active sites, which can offset the reduction in activity from the decreased surface area. In the case of the impregnated catalysts in our study, this loss of surface area and pore volume did not result in any loss of activity, as it will be discussed later in Section 3.3. On the contrary, increased formation of non-condensable gases was observed, which was an indication of increased catalyst activity, attributed to the generation of new active sites on the impregnated catalysts.

The XRD patterns of the HZSM-5 and SBA-15 catalysts are shown in Fig. 2a and b, respectively. XRD profiles showed that all HZSM-5 samples exhibited the typical peaks of MFI type zeolite at ~8° and 23° (Zhou et al., 2014), so the framework of ZSM-5 was preserved after Co and Ni impregnation. The Co-modified catalyst exhibited XRD patterns with the characteristic peaks of cobalt (II, III) oxide (Co<sub>3</sub>O<sub>4</sub>) (19°, 37°, 55°). Characteristic peaks belonging to cobalt (II) oxide (CoO) species were not detected, which was expected since the samples had undergone air calcination as mentioned above. Similar observations were recorded for the Ni-HZSM-5 catalyst. The catalyst exhibited the characteristic nickel (II) oxide (NiO) peaks at around 37° and 43°. The XRD patterns of SBA-15 samples exhibited the characteristic peaks of SBA-15 indexed to [100] at 0.5°, which indicated that the synthetic metal loaded SBA-15 (Me/SBA-15) catalysts maintained the ordered

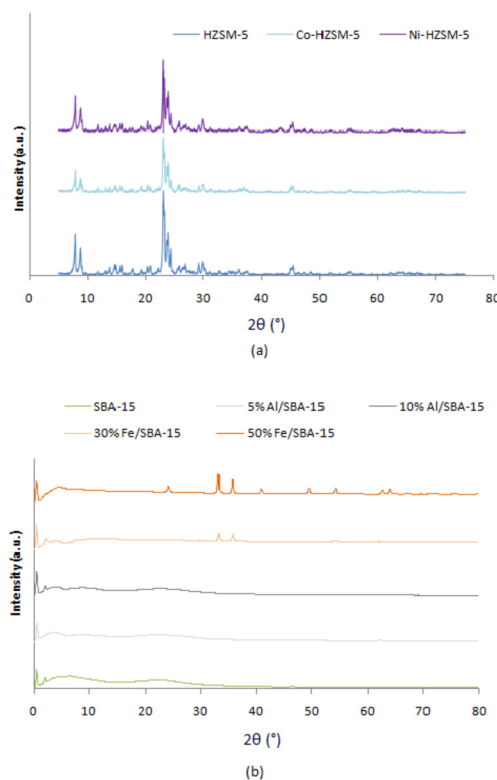


**Fig. 2.** XRD patterns of (a) HZSM-5, 5 wt% Co/HZSM-5 and 5 wt% Ni/HZSM-5, (b) SBA-15, 5 wt% Al/SBA-15, 10 wt% Al/SBA-15, 30 wt% Fe/SBA-15 and 50 wt% Fe/SBA-15.

hexagonal mesostructure of the SBA-15 material (Zhang et al., 2014). Moreover, the diffraction peaks of the Me/SBA-15 catalysts shifted to higher 2θ degrees, which might be because of the constriction of the framework (Lu et al., 2010a). No diffraction peaks from Al were detected, which might be due to too low Al content and the good dispersion of Al over the parent SBA-15. The Fe/SBA-15 catalyst showed the characteristic peaks of iron (III) oxide (Fe<sub>2</sub>O<sub>3</sub>) structure (24°, 33°, 36°, 40°, 49°, 54°, 62°, 64°). Fe<sub>2</sub>O<sub>3</sub> peak intensities increased with increasing Fe loading ratio.

### 3.3. Effects of catalysts on product yields and contents of biomass pyrolysis vapours

Results for the yields of bio-oil, water, organics, gases and solids from the non-catalytic and catalytic experimental runs are given in

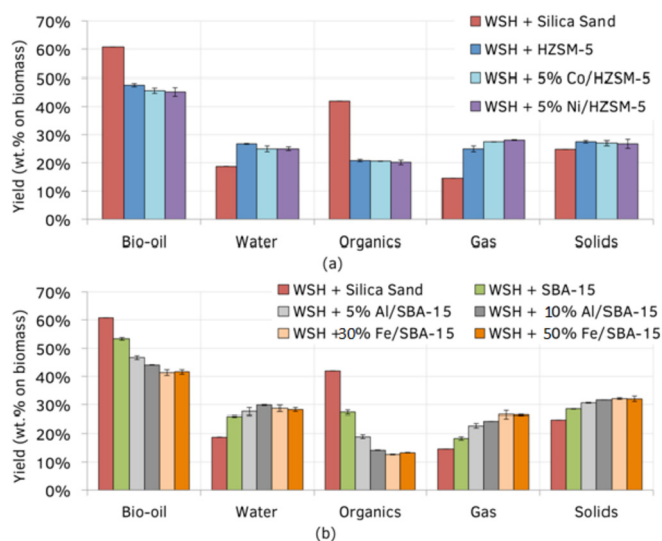


**Fig. 3.** Yields of pyrolysis products from the non-catalytic and catalytic pyrolysis of WSH with (a) HZSM-5 and (b) SBA-15 catalysts.

**Fig. 3.** As expected, the highest yields of bio-oil and organic fraction (60.7 wt% and 41.9 wt% respectively) were obtained in the absence of a catalyst. Char (solid product) yield was 24.8 wt%, while incondensable gas yield was 14.5 wt%. When the reactor was loaded with catalyst, cracking, dehydration, decarboxylation and decarbonylation reactions were catalyzed. As a result, an increase in the formation of water, gases and solid products was observed with all catalysts tested, at the expense of liquid organic product yield. The increased solid product yields were due to the formation of coke on the surface of the catalyst.

The parent mesoporous SBA-15 catalyst yielded markedly less water and gases than the parent microporous HZSM-5 and thus was less active in the conversion of the pyrolysis vapours, despite its higher surface area and its significantly larger sized pores. This was attributed to its lack of strong acidity compared to the HZSM-5, as SBA-15 was a purely siliceous material. Despite its lower activity however, SBA-15 was more prone to coke formation (solid product) and exhibited higher solid product yields (28.5 wt%) than the more active HZSM-5 (27.5 wt%). Coke formation is especially undesirable as it binds carbon in the solid byproduct and results in decreased organic bio-oil yields with low C/O ratios (Stefanidis et al., 2011a). Considering the lack of strong acidity in the SBA-15, coke formation was likely a result of the reactive species in the pyrolysis vapours coming in contact with the hot surface of the catalyst and repolymerising to form large structures that deposited as coke. The large pores of the SBA-15 allowed the formation of such large molecules, in contrast to the shape-selective micropore network of the HZSM-5 catalyst, which is known to inhibit coke formation (Jae et al., 2011).

Impregnation of the HZSM-5 with Co or Ni resulted in increased formation of gas products and reduced formation of water, indicating that the presence of metals shifted the deoxygenation mechanism of the catalyst from dehydration to decarbonylation and decarboxylation. Solid and liquid organic product yields were not significantly affected and any variations observed were within the experimental error. On the other hand, impregnation of SBA-15 with Al or Fe resulted in clearly higher catalyst activity and an increase in both water and gas yields were observed. Solid product yields also increased due to enhanced coke formation and as a result of all of the above; there was a marked decrease of the liquid organic product yields for all impregnated SBA-15 catalysts.

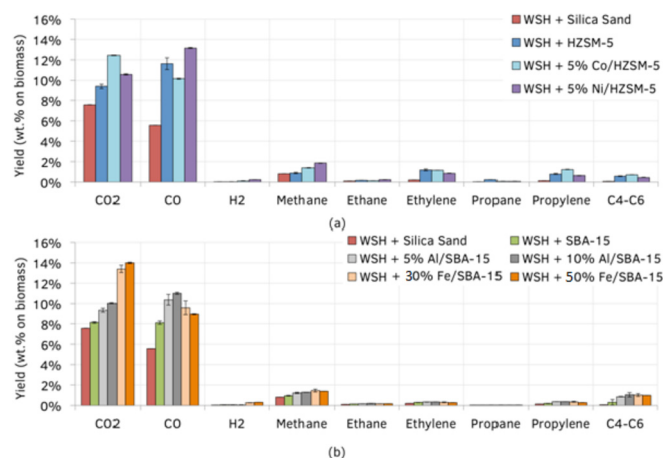


**Fig. 4.** Yields of gas products from the non-catalytic and catalytic pyrolysis of WSH with (a) HZSM-5 and (b) SBA-15 catalysts.

Increasing Al loading on the SBA-15 catalyst from 5 wt% to 10 wt% resulted in enhanced catalyst activity, while increasing Fe loading from 30 wt% to 50 wt% did not significantly affect the pyrolysis product yields.

Yields of evolved gases such as carbon dioxide (CO<sub>2</sub>), carbon monoxide (CO), hydrogen (H<sub>2</sub>), methane (CH<sub>4</sub>) and other light hydrocarbons for each catalyst used are given in Fig. 4. The main gas products in the absence of a catalyst were CO<sub>2</sub> (7.6 wt%) and CO (5.6 wt%). With the use of either HZSM-5 or SBA-15, CO<sub>2</sub> yield moderately increased compared to thermal pyrolysis, while CO formation increased more substantially. The presence of metals on the HZSM-5 enhanced gas formation. In the case of Co, this resulted in significant increase in CO<sub>2</sub> formation, while in the case of Ni, both CO<sub>2</sub> and CO formation was enhanced. Accordingly, the presence of Al on the SBA-15 catalyst enhanced CO formation, while the presence of Fe greatly increased CO<sub>2</sub> yields. The higher production of CO<sub>2</sub> was indicative of the different decarbonylation/decarboxylation mechanism that was promoted by Co/HZSM-5 and Fe/SBA-15 compared to the parent HZSM-5 and SBA-15 respectively, due to the differences in their acidic properties (Iliopoulou et al., 2012). Methane and C<sub>4</sub>-C<sub>6</sub> gaseous alkanes were also present in the gas products, as well as H<sub>2</sub> in very small amounts.

The elemental composition of the organic fraction of the bio-oils is given in Table 3. Highly oxygenated bio-oil was observed from the non-catalytic pyrolysis of WSH (40.6 wt% oxygen content). Utilizing catalysts led to reduction in the oxygen content of the organic fraction due to oxygen transfer to the gas products (CO and CO<sub>2</sub>) and water. The most deoxygenated bio-oil was produced with the parent HZSM-5 catalyst (33.5 wt% oxygen content). On the other hand, the oxygen content of the bio-oil was only marginally reduced with the parent SBA-15 catalyst (39.1 wt%), despite the obvious removal of oxygen via formation of water, CO<sub>2</sub> and CO (see Fig. 4b). This was attributed to the overall low activity of the SBA-15, combined with its high affinity for coke formation (see Fig. 3), which removed carbon from the pyrolysis vapours and resulted in low C/O ratio in the condensable products. Ni or Co promoted HZSM-5 gave bio-oil with similar oxygen content, which was higher than what was observed with the parent HZSM-5, between 34.9 and 35.1 wt%. It was evident that the shift of the oxygen removal mechanism from formation of water to formation of CO and CO<sub>2</sub> (see Figs. 3b and 4b) with the metal promoted HZSM-5 catalysts was not beneficial for the reduction of the bio-oil's oxygen content. Contrary to what was observed with the HZSM-5 catalysts, the incorporation of metals on the siliceous SBA-15

**Table 3**  
Elemental composition of the organic fraction of the bio-oils from non-catalytic and catalytic pyrolysis of WSH with HZSM-5 and SBA-15 catalysts.

	Organics yield (wt.% on biomass)	C In organics (wt.%)	H In organics (wt.%)	O In organics <sup>a</sup> (wt.%)
WSH + Sand	41.9	53.1	6.2	40.6
WSH + HZSM-5	20.9 ± 0.4	59.2 ± 0.8	7.3 ± 0.4	33.5 ± 1.1
WSH + Co-HZSM-5	20.6 ± 0.1	57.9 ± 0.9	7.2 ± 0.1	34.9 ± 0.8
WSH + Ni-HZSM-5	20.2 ± 0.9	57.6 ± 0.2	7.3 ± 0.1	35.1 ± 0.3
WSH + SBA-15	27.4 ± 0.8	53.6 ± 0.2	7.4 ± 0.0	39.1 ± 0.2
WSH + 5% Al/SBA-15	19.0 ± 0.7	58.2 ± 1.2	7.6 ± 0.2	34.2 ± 0.9
WSH + 10% Al/SBA-15	14.2 ± 0.1	55.2 ± 1.2	7.6 ± 0.1	37.2 ± 1.1
WSH + 30% Fe/SBA-15	12.6 ± 0.1	57.2 ± 0.5	7.3 ± 0.6	35.5 ± 0.2
WSH + 50% Fe/SBA-15	13.3 ± 0.1	56.7 ± 0.1	7.3 ± 0.3	35.9 ± 0.4

<sup>a</sup> By difference.

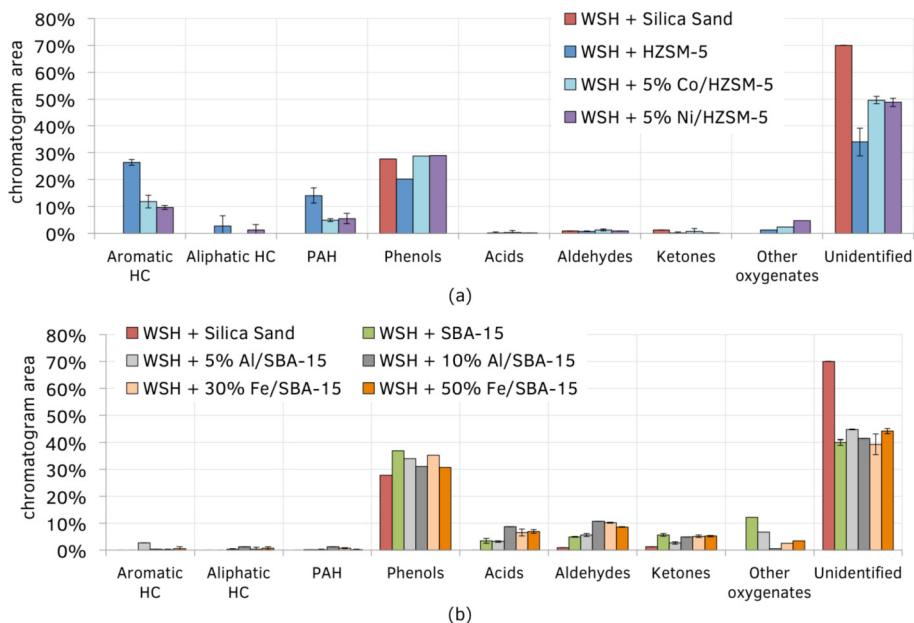


**Fig. 5.** Chemical composition of the organic fraction of bio-oils from non-catalytic and catalytic pyrolysis with (a) HZMS-5 and (b) SBA-15 catalysts.

catalyst resulted in clearly enhanced activity and removal of oxygen via both water and gas formation, which ultimately resulted in less oxygenated bio-oils compared to the parent SBA-15.

The qualitative composition data of the bio-oil's organic fraction from GC-MS analysis are given in Fig. 5. The identified compounds were classified into 8 groups; aromatic hydrocarbons, aliphatic hydrocarbons, polycyclic aromatic hydrocarbons (PAH), phenols, acids, aldehydes, ketones and other oxygenates (furans, esters, ethers, alcohols etc.). Compounds that could not be identified by the GC-MS system were classified as unidentified. Based on their commercial value and on their effect on the properties of the bio-oil, compounds can be considered as desirable or undesirable. For example, acids can be considered undesirable because they contribute to the corrosivity of the bio-oil. Ketones and aldehydes are reactive compounds and reduce its stability. Esters, ethers and oxygenates in general reduce its heating value, while PAHs are hazardous because of their carcinogenic potential. On the other hand, phenols and aromatic hydrocarbons are high added value products that can be considered desirable for the production of fuels and chemical products. A more detailed view of the composition of the phenolic compounds in the non-catalytic and catalytic bio-oil of this study is given in Fig. 6.

The bio-oil from the non-catalytic pyrolysis of WSH was composed primarily of phenols and more specifically, guaiacyl-type

and syringyl-type compounds, which were derived from the thermal decomposition of the WSH's lignin fraction. Many other peaks appeared in the chromatogram of the non-catalytic bio-oil that could not be identified by the GC-MS system, a significant portion of which (about 33% of the total chromatogram area) was attributed to heavier compounds that appeared at high retention times. The bio-oil from non-catalytic pyrolysis also contained low amounts of alkylated phenols and catechol-type compounds, which were formed from guaiacyl- and syringyl-type compounds via secondary thermal reactions (Asmadi et al., 2011).

With the parent HZSM-5, total phenols and unidentified compounds were reduced and a significant formation of aromatic hydrocarbons, PAH and phenols was observed. More specifically, syringyl- and guaiacyl-type compounds in the bio-oil were reduced, while alkylated phenols increased. The heavier unidentified compounds were also reduced, from about 33% in the non-catalytic bio-oil to about 17%. It appears that the guaiacyl- and syringyl-type compounds in the pyrolysis vapours from the decomposition of WSH were converted to alkylated phenols and hydrocarbons with the ZSM-5 catalyst. It is also possible that the external surface acidity of the HZSM-5 zeolite catalysed the cracking of the heavy molecules in the pyrolysis vapours into smaller ones, which in turn entered the small catalyst pores of the zeolite and converted to aromatic hydrocarbons and PAHs via aromatization reactions (Lu et al., 2010b).

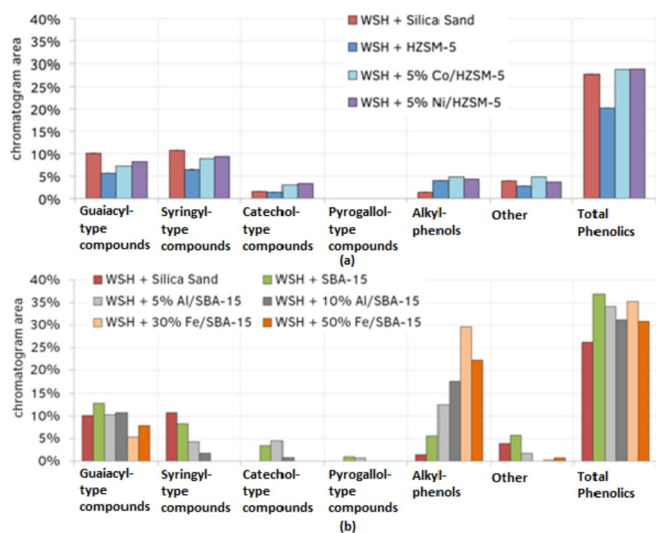


Fig. 6. Composition of the phenols in the organic fraction of the bio-oil from non-catalytic and catalytic pyrolysis of WSH with (a) HZSM-5 and (b) SBA-15 catalysts.

The selectivity results were found to be similar to those reported in the literature (Heo et al., 2011; Zhang et al., 2009). With either Co/HZSM-5 or Ni/HZSM-5, this effect was mitigated. Compared to the parent HZSM-5, the impregnated catalysts yielded more syringyl-type, guaiacyl-type and unidentified compounds (heavy compounds around 22% and 19% for Co/HZSM-5 and Ni/HZSM-5 respectively), while the formation of aromatic hydrocarbons and PAHs was markedly reduced. Instead, formation of alkylated phenols and catechol-type compounds appeared to be enhanced. It is possible that the impregnated metals reduced the acidity of the HZSM-5 by masking the acid sites and as such, cracking and aromatization activity was reduced with the impregnated catalysts. In a recent study, To and Resasco (2014) suggested that phenolic compounds adsorb on the acid sites of the catalyst and form multiphenyl species via condensation, producing water. Aromatic hydrocarbons were suggested to be formed not from the direct deoxygenation of the phenolic compounds, but from the cracking of these multi-phenyl species. Our results seem to be in agreement with the suggested mechanism as, when the acid sites of the catalyst were masked by the impregnated metals, reduced formation of aromatic hydrocarbons was observed, along with reduced water formation.

With the parent SBA-15 catalyst, the heavier unidentified compounds that were observed in non-catalytic pyrolysis were completely eliminated from the chromatogram and an increase in the total phenolic compounds was observed, along with an increase in acids, aldehydes and ketones. It seems that introduction of the mesoporous SBA-15 catalyst facilitated the cracking of the heavier molecules that were produced from the thermal decomposition of lignin to phenolic monomers and other small oxygenates. Guaiacyl-type compounds in the bio-oil after catalysis with the SBA-15 catalyst increased, while syringyl-type compounds, which are more reactive (Asmadi et al., 2011), slightly decreased. Alkylated phenols were formed, as well as catechol- and pyrogallols-type compounds from the conversion of guaiacyl- and syringyl-type compounds (Fig. 6).

With the impregnation of metals on the SBA-15, the catalyst's activity increased as already mentioned. Small oxygenates such as aldehydes and acids increased, tentatively due to the more effective cracking of heavier molecules and greater conversion of guaiacyl- and syringyl-type compounds was observed, possibly attributed to

the Lewis acid sites formed after metal impregnation. It is noteworthy that after impregnation with metals, the selectivity of the SBA-15 appeared to shift from catechol- and pyrogallol-type compounds to alkylated phenols, especially at 10% Al, 30% Fe and 50% Fe metal loadings. With these materials, formation of catechol- and pyrogallols-type compounds was significantly reduced, while formation of alkylated phenols increased remarkably. Ma et al. (2012) have found that large molecule conversion depends on two catalyst properties, acidity and pore size. They found that a porous catalyst that lacked acidity produced more bio-oil from lignin pyrolysis without converting it further. On the other hand, an acidic microporous catalyst (H-ZSM-5) was able to convert lignin to aromatic hydrocarbons following the scheme lignin oligomers  $\rightarrow$  alkoxy phenols  $\rightarrow$  phenols  $\rightarrow$  aromatic hydrocarbons. They also found that low Si/Al catalysts were more acidic and hence more efficient at converting alkoxy phenols. However, microporous catalysts such as ZSM-5 required high temperatures in order to decrease the energy barrier of diffusion of large molecules such as lignin oligomers, within the catalyst pores. In this work, the parent SBA-15 had large pores suitable for the conversion of large molecules from the lignin fraction of WSH but lacked the necessary acidity to efficiently convert and deoxygenate them further. Adding Al or Fe, increased catalyst acidity, which combined with its mesopores led to significant conversion of the alkoxy phenols to more deoxygenated products such as alkyl phenols.

As mentioned before, different trends are observed for the HZSM-5 catalysts compared to the SBA-15. Comparing silica sand to parent HZSM-5, the guaiacyl- and syringyl-type compounds that are formed from the thermal decomposition of the lignin fraction in the WSH are markedly reduced and are apparently converted mainly to alkylated phenols and aromatic and polyaromatic hydrocarbons. Based on the above observations, a reaction scheme for the thermal decomposition and catalytic upgrading of the WSH is presented in Fig. 7.

### 3.4. Preliminary techno-economic analysis

In order to estimate the investment and operating cost of a walnut shell catalytic pyrolysis process, the data from this work were imported in a techno-economic model that was developed and reported by Vasalos et al. (2016). Considering the annual production of about 136,150 metric tonnes (t) of walnut shell in Turkey in 2012 (Uzun and Yaman, 2014), a walnut shell catalytic pyrolysis plant with a capacity of 135,000 t/y was assumed, producing 27,309 t/y of organic catalytic pyrolysis oil (CPO). Scoping investment costs were estimated using real costs of a Fluid Catalytic Cracking Unit (FCCU), due to the similarity of the two processes. The Inside Battery Limits (ISBL) investment cost of the FCCU was broken down to several sections and appropriate scale up parameters was used for estimating the walnut shell catalytic pyrolysis plant costs. The ISBL cost was estimated at about 39.3 MM 2012 US\$ and the total investment cost at about 81.9 MM 2012 US\$. Utility costs were estimated by scaling up with capacity similar costs from an FCC unit. Labour costs were estimated from information received for similar units operating in Canada and the United States, while catalyst usage was projected based on residue processing practices. Assuming an average price of 57 US\$ per dry t for the walnut shell, the cost of the CPO production was estimated at 771 US\$/t. If walnut shell is considered a waste feedstock that can be acquired at zero price, the cost of CPO production can be reduced to 468 US\$/t.

The CPO production cost predicted from this preliminary techno-economic analysis is markedly higher than the CPO production cost that was reported by Vasalos et al. (2016) when considering a wood biomass feedstock. The main reason for the increased production cost is lower yield of CPO for walnut shell in

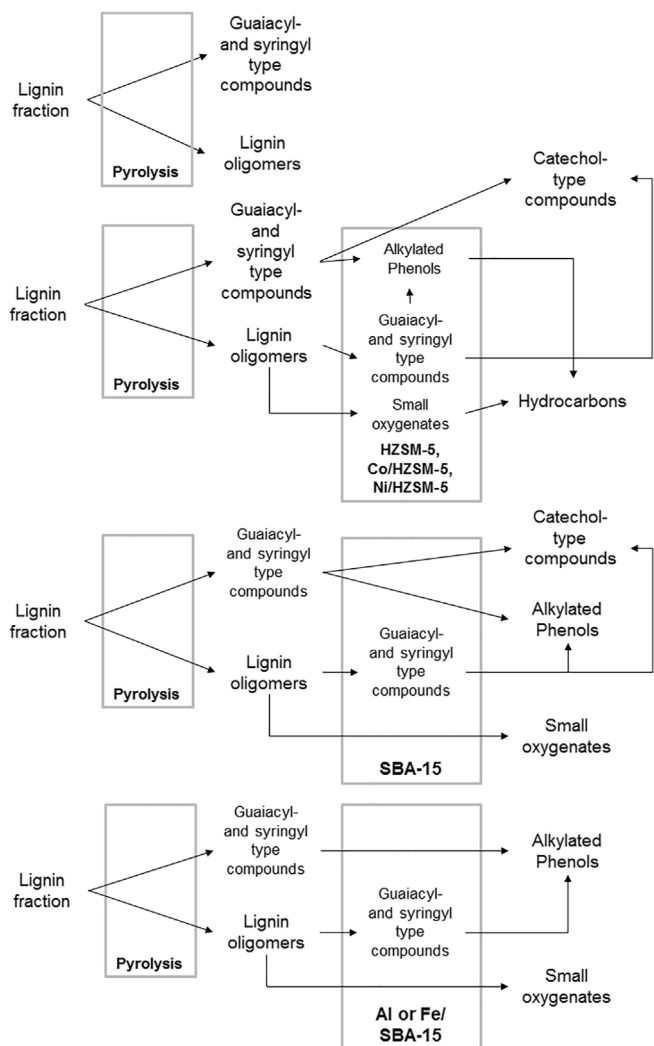


Fig. 7. Reaction scheme for the thermal decomposition and catalytic upgrading of pyrolysis vapours from WSH with HZSM-5 and SBA-15 catalysts.

this study, compared to wood biomass. It must be stressed however that the walnut shell catalytic pyrolysis data in this work were obtained from experiments at the lab-scale, while the data used by Vasalos et al. (2016) were obtained from pilot-scale experiments, which are more representative of a commercial scale process.

#### 4. Conclusions

The aim of the study was to investigate the effects of catalyst support and impregnated metal type on the bio-oil composition in terms of phenolic fractions. For this purpose, in-situ upgrading of WSH pyrolysis vapours over HZSM-5, Ni/HZSM-5, Co/HZSM-5, SBA-15, Al/SBA-15, and Fe/SBA-15 was performed in a fixed bed reactor to improve the alkylated phenols in bio-oil as a source of various applications. The textural properties of catalyst were affected as surface area and pore volume decreased. These catalysts were evaluated according to organic liquid product yield, deoxygenation ability and selectivity towards desirable products. Catalytic biomass pyrolysis produced high coke and gas yields (with the oxygenated gaseous compounds of CO<sub>2</sub> and CO being superior) compared to non-catalytic pyrolysis in contrast to decrease in organic phase in the produced bio-oil. Decreased organic fractions specified that water production increased due to the catalytic reactions in the

presence of HZSM-5 and SBA-15 materials. Both non-catalytic and catalytic bio-oils had high content in phenolic compounds. However, it seemed that introduction of HZSM-5 and SBA-15 catalysts reduced the heavier compounds that were produced from the thermal decomposition of lignin and guaiacyl-, syringyl- and catechol-type compounds were formed, along with alkylated phenols and other small oxygenates (acids, ketones, aldehydes). With the introduction of metals in the catalyst, selectivity to alkylated phenols was increased (especially with 5% Co HZSM-5, 10% Al, 30% Fe and 50% Fe SBA-15). As a result, metal impregnated HZSM-5 and SBA-15 materials could be utilized to enhance deoxygenation of lignin produced bio-oil and selectively increase the phenolic content of the bio-oil for the production of value added chemicals. According to the preliminary economic analysis, the cost of the catalytic pyrolysis oil production from walnut shell was predicted as 771 US\$/t. Walnut shell can be provided as waste feedstock that can be obtained at zero price, the cost of pyrolysis oil production can be reduced to 468 US\$/t.

#### Acknowledgements

The authors acknowledge the financial support provided by Biofuels Research Infrastructure for Sharing Knowledge (BRISK) Projects through the European Commission Seventh Framework Programme with project no: 160-CER1 and project title: "Effect of Metal Loaded Catalysts on Phenolic Content of Bio-Oil"; and project no:166-CER1 and project title: "Catalytic Pyrolysis of Biomass".

#### References

- Asmadi, M., Kawamoto, H., Saka, S., 2011. Thermal reactions of guaiacol and syringol as lignin model aromatic nuclei. *J. Anal. Appl. Pyrol* 92 (1), 88–98.
- Aysu, T., 2015. Catalytic pyrolysis of *Eremurus spectabilis* for bio-oil production in a fixed-bed reactor: effects of pyrolysis parameters on product yields and character. *Fuel Process. Technol.* 129, 24–38.
- Balasundram, V., Ibrahim, N., Kasmani, R.M., Hamid, M.K.A., Isha, R., Hasbullah, H., Ali, R.R., 2017. Thermogravimetric catalytic pyrolysis and kinetic studies of coconut copra and rice husk for possible maximum production of pyrolysis oil. *J. Clean. Prod.* 167, 218–228.
- David, G.F., Perez, V.H., Justo, O.R., Garcia-Perez, M., 2017. Effect of acid additives on sugarcane bagasse pyrolysis: production of high yields of sugars. *Bioresour. Technol.* 223, 74–83.
- French, R., Czernik, S., 2010. Catalytic pyrolysis of biomass for biofuels production. *Fuel Process. Technol.* 91, 25–32.
- Gomez, N., Rosas, J.G., Cara, J., Martinez, O., Alburquerque, J.A., Sanchez, M.E., 2016. Slow pyrolysis of relevant biomasses in the Mediterranean basin. Part 1. Effect of temperature on process performance on a pilot scale. *J. Clean. Prod.* 120, 181–190.
- Harker, J.H., Backhurst, J.R., 1981. *Fuel and Energy*. Academic Press Limited, London.
- Hassan, E.B., Abou-Yousef, H., Steele, P., El-Giar, E., 2016. Characterization of bio-oils from the fast pyrolysis of white oak and sweetgum. *Energy. Source. Part A* 38, 43–50.
- Heo, H.S., Kim, S.G., Jeong, K.E., Jeon, J.K., Park, S.H., Kim, J.M., Kim, S.S., Park, Y.K., 2011. Catalytic upgrading of oil fractions separated from food waste leachate. *Bioresour. Technol.* 102, 3952–3957.
- Huber, G.W., Iborra, S., Corma, A., 2006. Synthesis of transportation fuels from biomass: chemistry, catalysts, and engineering. *Chem. Rev.* 106, 4044–4098.
- Iliopoulou, E.F., Stefanidis, S.D., Kalogiannis, K.G., Delimitis, A., Lappas, A.A., Triantafyllidis, K.S., 2012. Catalytic upgrading of biomass pyrolysis vapors using transition metal-modified ZSM-5 zeolite. *Appl. Catal. B* 127, 281–290.
- Iliopoulou, E.F., Stefanidis, S., Kalogiannis, K., Psarras, A.C., Delimitis, A., Triantafyllidis, K.S., Lappas, A.A., 2014. Pilot scale validation of CoZSM5 catalyst performance in the catalytic upgrading of biomass pyrolysis vapours. *Green Chem.* 16, 662–674.
- Iranmahboob, J., Nadim, F., Monemi, S., 2002. Optimizing acid hydrolysis: a critical step for production of ethanol from mixed wood chips. *Biomass Bioenergy* 22, 401–404.
- Jae, J., Tompsett, G.A., Foster, A.J., Hammond, K.D., Auerbach, S.M., Lobo, R.F., Huber, G.W., 2011. Investigation into the shape selectivity of zeolite catalysts for biomass conversion. *J. Catal.* 279, 257–268.
- Jeon, M.J., Jeon, J.K., Suh, D.J., Park, S.H., Sa, Y.J., Joo, S.H., Park, Y.K., 2013. Catalytic pyrolysis of biomass components over mesoporous catalysts using Py-GC/MS. *Catal. Today* 204, 170–178.
- Kumagai, S., Matsuno, R., Grause, G., Kameda, T., Yoshioka, T., 2015. Enhancement of bio-oil production via pyrolysis of wood biomass by pretreatment with H<sub>2</sub>SO<sub>4</sub>.

- Bioresour. Technol. 178, 76–82.
- Kumar, P., Barret, D.M., Delwiche, M.J., Stroeve, P., 2009. Methods for pre-treatment of lignocellulosic biomass for efficient hydrolysis and biofuel production. *Ind. Eng. Chem. Res.* 48, 3713–3729.
- Lappas, A.A., Kalogiannis, K.G., Iliopoulou, E.F., Triantafyllidis, K.S., Stefanidis, S.D., 2012. Catalytic pyrolysis of biomass for transportation fuels. *WIREs Energy Environ.* 1, 285–297.
- Lim, C.H., Mohammed, I.Y., Abakr, Y.A., Kazi, F.K., Yusup, S., Lam, H.L., 2016. Novel input-output prediction approach for biomass pyrolysis. *J. Clean. Prod.* 136, 51–61.
- Lu, Q., Tang, Z., Zhang, Y., Zhu, X.F., 2010a. Catalytic upgrading of biomass fast pyrolysis vapors with Pd/SBA-15 catalysts. *Ind. Eng. Chem. Res.* 49, 2573–2580.
- Lu, Q., Zhang, Y., Tang, Z., Li, W.Z., Zhu, X.F., 2010b. Catalytic upgrading of biomass fast pyrolysis vapors with titania and zirconia/titania based catalysts. *Fuel* 89, 2096–2103.
- Ma, Z., Troussard, E., van Bokhoven, J.A., 2012. Controlling the selectivity to chemicals from lignin via catalytic fast pyrolysis. *Appl. Catal. A-Gen.* 423–424, 130–136.
- Mohammed, I.Y., Abakr, Y.A., Musa, M., Yusup, S., Singh, A., Kazi, F.K., 2016. Valorization of Bambara groundnut shell via intermediate pyrolysis: products distribution and characterization. *J. Clean. Prod.* 139, 717–728.
- Mohammed, I.Y., Abakr, Y.A., Yusup, S., Kazi, F.K., 2017. Valorization of Napier grass via intermediate pyrolysis: optimization using response surface methodology and pyrolysis products characterization. *J. Clean. Prod.* 142, 1848–1866.
- Mourant, D., Wang, Z., He, M., Wang, X.S., Garcia-Perez, M., Ling, K., Li, C.-Z., 2011. Mallee wood fast pyrolysis: effects of alkali and alkaline earth metallic species on the yield and composition of bio-oil. *Fuel* 90, 2915–2922.
- Ning, S.K., Hung, M.C., Chang, Y.H., Wan, H.P., Lee, H.T., Shih, R.F., 2013. Benefit assessment of cost, energy, and environment for biomass pyrolysis oil. *J. Clean. Prod.* 59, 141–149.
- Oasmaa, A., Czernik, S., 1999. Fuel oil quality of biomass pyrolysis oils state of the art for the end users. *Energ. Fuel* 13, 914–921.
- Ozbay, N., Yargic, A.S., Yarbay Sahin, R.Z., 2017. Tailoring Cu/Al<sub>2</sub>O<sub>3</sub> catalysts for the catalytic pyrolysis of tomato waste. *J. Energy Inst.* (in press).
- Pirayesh, H., Khanjanzadeh, H., Salari, A., 2013. Effect of using walnut/almond shells on the physical, mechanical properties and formaldehyde emission of particleboard. *Compos. Part B-Eng* 45, 858–863.
- Pittman, C.U., Mohan, D., Eseyin, A., Li, Q., Ingram, L., Hassan, E.B.M., Mitchell, B., Guo, H., Steele, P.H., 2012. Characterization of bio-oils produced from fast pyrolysis of corn stalks in an auger reactor. *Energ. Fuel* 26, 3816–3825.
- Qiang, L., Wen-zhi, L., Dong, Z., Xi-feng, Z., 2009. Analytical pyrolysis–gas chromatography/mass spectrometry (Py–GC/MS) of sawdust with Al/SBA-15 catalysts. *J. Anal. Appl. Pyrol* 84, 131–138.
- Stefanidis, S.D., Kalogiannis, K.G., Iliopoulou, E.F., Lappas, A.A., Pilavachi, P.A., 2011a. In-situ upgrading of biomass pyrolysis vapors: catalyst screening on a fixed bed reactor. *Bioresour. Technol.* 102, 8261–8267.
- Stephanidis, S., Nitsos, C., Kalogiannis, K., Iliopoulou, E.F., Lappas, A.A., Triantafyllidis, K.S., 2011b. Catalytic upgrading of lignocellulosic biomass pyrolysis vapors: effect of hydrothermal pre-treatment of biomass. *Catal. Today* 167, 37–45.
- Stefanidis, S.D., Heracleous, E., Th Patiaka, D., Kalogiannis, K.G., Michailof, C.M., Lappas, A.A., 2015. Optimization of bio-oil yields by demineralization of low quality biomass. *Biomass Bioenerg.* 83, 105–115.
- To, A.T., Resasco, D.E., 2014. Role of a phenolic pool in the conversion of m-cresol to aromatics over HY and HZSM-5 zeolites. *Appl. Catal. A-Gen* 487, 62–71.
- Uzun, B.B., Sarioglu, N., 2009. Rapid and catalytic pyrolysis of corn stalks. *Fuel Process. Technol.* 90, 705–716.
- Uzun, B.B., Apaydin-Varol, E., Ateş, F., Özbay, N., Pütün, A.E., 2010. Synthetic Fuel Production from tea waste: Characterisation of bio-oil and bio-char. *Fuel* 89, 176–184.
- Uzun, B.B., Yaman, E., 2014. Thermogravimetric characteristics and kinetics of scrap tyre and Juglans regia shell co-pyrolysis. *Waste Manage* 32, 961–970.
- Vasalos, I.A., Lappas, A.A., Kopalidou, E.P., Kalogiannis, K.G., 2016. Biomass catalytic pyrolysis: process design and economic analysis. *WIREs Energy Environ.* 5, 370–383.
- Zhai, M., Shi, G., Wang, Y., Mao, G., Wang, D., Wang, Z., 2015. Chemical compositions and biological activities of pyrolytic acids from walnut shell. *Bioresources* 10, 1715–1729.
- Zhang, H., Xiao, R., Huang, H., Xiao, G., 2009. Comparison of non-catalytic and catalytic fast pyrolysis of corncob in a fluidized bed reactor. *Bioresour. Technol.* 100, 1428–1434.
- Zhang, Y., Xiao, R., Gu, X., Zhang, H., Shen, D., He, G., 2014. Catalytic pyrolysis of biomass with Fe/La/SBA-15 catalyst using TGA-FTIR analysis. *Bioresources* 9, 5234–5245.
- Zhou, S., Wang, Z., Liaw, S.S., Li, C.Z., Garcia-Perez, M., 2013a. Effect of sulfuric acid on the pyrolysis of Douglas fir and hybrid poplar wood: py-GC/MS and TG studies. *J. Anal. Appl. Pyrol* 104, 117–130.
- Zhou, Z., Mourant, D., Lievens, C., Wang, Y., Li, C., Garcia-Perez, M., 2013b. Effect of sulfuric acid concentration on the yield and properties of the bio-oils obtained from the auger and fast pyrolysis of Douglas fir. *Fuel* 104, 536–546.
- Zhou, G., Li, J., Yu, Y., Li, X., Wang, Y., Wang, W., Komarneni, S., 2014. Optimizing the distribution of aromatic products from catalytic fast pyrolysis of cellulose by ZSM-5 modification with boron and co-feeding of low-density polyethylene. *Appl. Catal. A-Gen* 487, 45–53.